Initial test results of an SRF cavity field and resonance controller based on DMD

LLRF Workshop 2023. Gyeongju, South Korea

Faya Wang & Jorge Diaz

24 October 2023

SLAC NATIONAL ACCELERATOR LABORATORY

Stanford University | U.S. DEPARTMENT OF ENERGY

CONTENT

Introduction

Motivation: For large machines like the LCLS-II, effective resonance control of superconducting RF cavities is critical, due to their high Q and narrow bandwidth, which make the SRF cavities sensitive to microphonics. Decrease RF power consumption, cryogenic heat loads and costs can be achieved by minimizing SRF cavity detuning due to microphonics.

Common sources of microphonics are helium pressure fluctuation, vacuum pumps, stochastic background noise, etc.

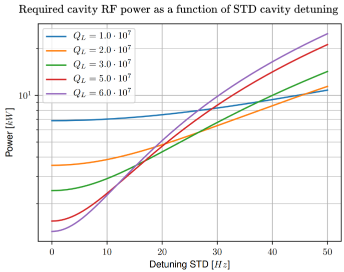

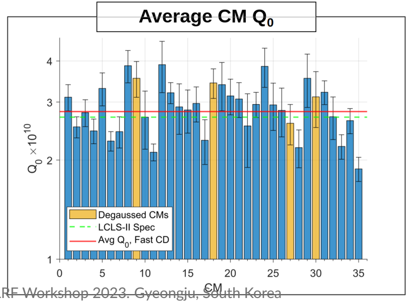

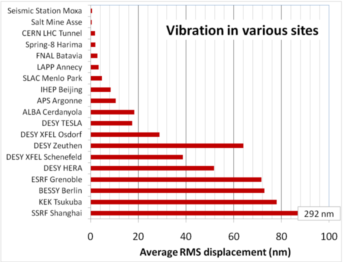

Introduction

In recent years, active resonance control (ARC) methods have been demonstrated at Fermilab, CBETA, DESY and SLAC. These methods are equivalent to notch filters, usually need the piezo tuner transfer function, and rely on well-calibrated dynamic models that require constant manual tuning and characterization by operators for each cavity.

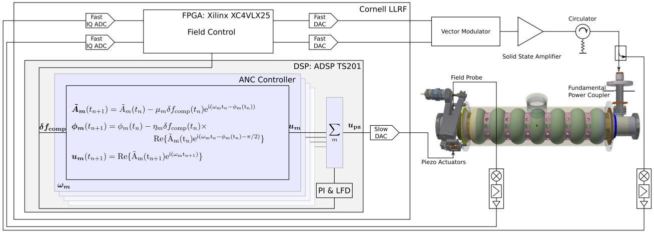

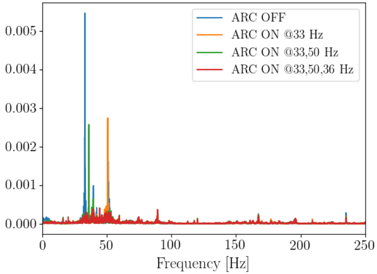

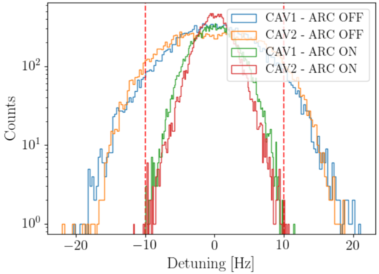

Banerjee, Nilanjan, et al. Physical Review Accelerators and Beams 22.5 (2019): 052002

Introduction

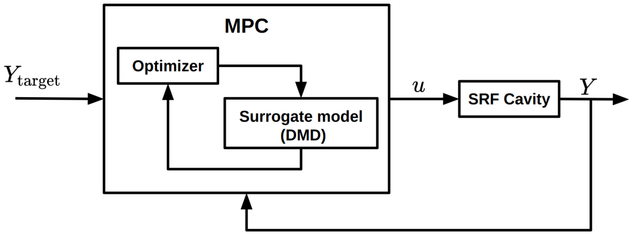

$$Y_{\text{target}} = [V_r \; V_i \; \Delta\omega]$$

$$u = \delta\omega$$

- Goal: Enhance SRF cavity stability and minimize SRF cavity detuning with a data-driven model predictive control (MPC) based on the dynamic mode decomposition (DMD) method.
- MPC allows us to incorporate learned models into control of individual cavities.
- DMD identifies a set of modes to generate system dynamics.
- We plan to implement MPC on an FPGA for resonance control

Introduction

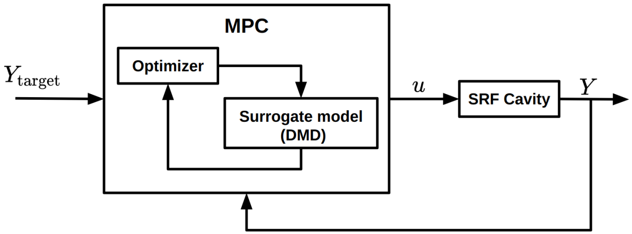

$$Y_{\text{target}} = [V_r \; V_i \; \Delta\omega]$$

$$u = \delta\omega$$

- Goal: Enhance SRF cavity stability and minimize SRF cavity detuning with a data-driven model predictive control (MPC) based on the dynamic mode decomposition (DMD) method.
- MPC allows us to incorporate learned models into control of individual cavities.
- DMD identifies a set of modes to generate system dynamics.
- We plan to implement MPC on an FPGA for resonance control
- Needs data to train the DMD model
- Computing burden is a concern when implementing MPC on an FPGA

Introduction

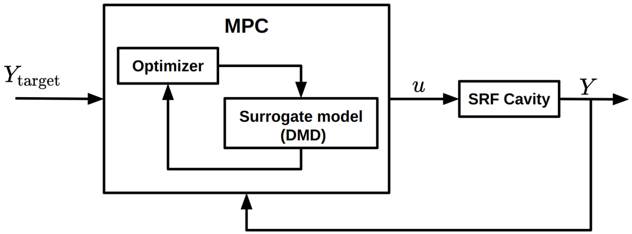

$$Y_{\text{target}} = [V_r \, V_i \, \Delta\omega]$$

$$u = \delta\omega$$

Plan:

- Simulation (MPC and DMD) ✔
- Data acquisition ✔
- Train the model (DMD) ✔
- Implement MPC controller
- Test MPC controller using cold cavities

This is a work in progress

Dynamic Mode Decomposition

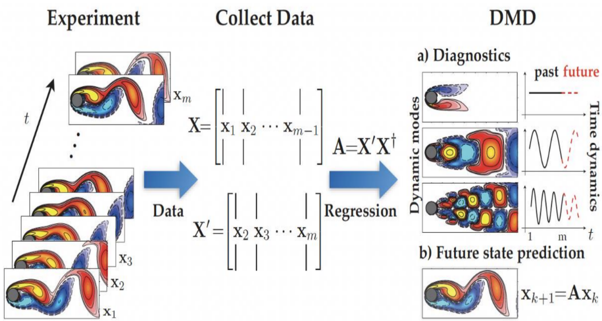

- The method originated in the fluid dynamics community in 2010 [1]
- Widely adopted due to the formulation as a linear regression problem based entirely on measurement data.
- We use the model to predict the future status of the system
- Traditional DMD is sensitive to noise, control inputs and nonlinearity. Multiple noise-robust approaches and DMD with control have been demonstrated. We base our implementation on the linear and nonlinear disambiguation optimization (LANDO) algorithm, which enables DMD in highly nonlinear and high-dimensional systems [2].

Dynamic Mode Decomposition

- Cavity state

$$x_k = \begin{bmatrix} V_{rk} & V_{ik} & \dot{V}_{rk} & \dot{V}_{ik} & \Delta\omega_k & \Delta\dot{\omega}_k \end{bmatrix}^{\mathsf{T}}$$

- Control signals

$$u_k = \begin{bmatrix} V_{grk} & V_{gik} & \delta\omega_k \end{bmatrix}^{\mathsf{T}}$$

- Relationship between system and control

$$x_{k+1} \approx \boldsymbol{A}x_k + \boldsymbol{B}u_k$$

$\boldsymbol{A}$ represents unforced system dynamics
$\boldsymbol{B}$ represents system's response to control inputs
Operator $\boldsymbol{B}$ is unkown, since the forced cavity system is complex and nonlinear

- With DMD, we can rewrite the system as

$$\boldsymbol{X}' = \boldsymbol{G}\tilde{\boldsymbol{X}}$$

$$\tilde{\boldsymbol{X}} = \begin{bmatrix} \boldsymbol{X} \\ \boldsymbol{U} \end{bmatrix}$$

$$\boldsymbol{G} = \begin{bmatrix} \boldsymbol{A} & \boldsymbol{B} \end{bmatrix}$$

where

$$\boldsymbol{X} = \begin{bmatrix} x_1 & x_2 & \cdots & x_m \end{bmatrix}$$

$$\boldsymbol{X}' = \begin{bmatrix} x_2 & x_3 & \cdots & x_{m+1} \end{bmatrix}$$

$$\boldsymbol{U} = \begin{bmatrix} u_1 & u_2 & \cdots & u_m \end{bmatrix}$$

Dynamic Mode Decomposition

- Using kernel methods, we can approximate the previous equation as

$$\boldsymbol{X}' \approx \boldsymbol{W}\boldsymbol{K}$$

- Polynomial kernel

$$\boldsymbol{K}_{i,j} = k(\tilde{x}_i, \tilde{x}_j) = \sum_d \alpha_d (\tilde{x}_i^T \tilde{x}_j)^d$$

Dynamic Mode Decomposition

- Using kernel methods, we can approximate the previous equation as

$$\boldsymbol{X'} \approx \boldsymbol{WK}$$

- Polynomial kernel

$$\boldsymbol{K}_{i,j} = k(\tilde{x}_i, \tilde{x}_j) = \sum_d \alpha_d (\tilde{x}_i^T \tilde{x}_j)^d$$

- The "almost linearly dependent" (ALD) test is used to reduce the size of the dictionary.

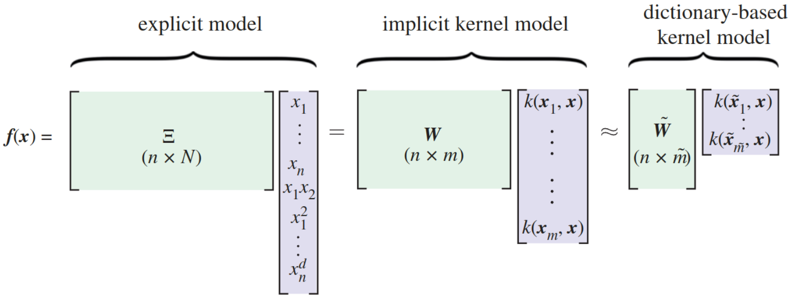

- The matrix of weights $\tilde{W}$ is solved using the pseudoinverse method. More details in [3]

Dynamic Mode Decomposition

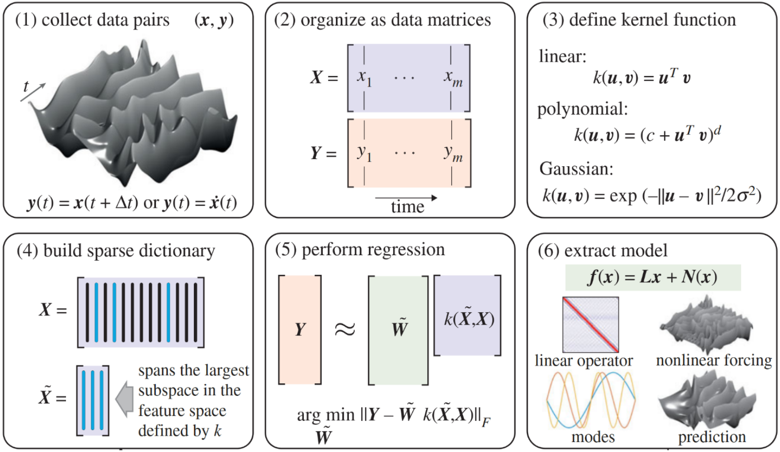

Peter J. Baddoo et al. Proceedings of the Royal Society A: Mathematical, Physical and Engineering Sciences 478.2260 (2022)

DMD predictions using simulated data

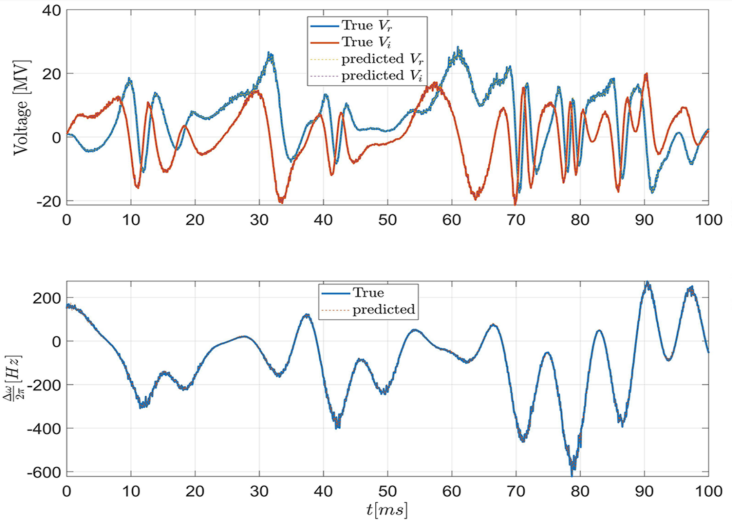

- Predicted cavity voltage vs true voltage. Real and imaginary components
- Predicted cavity detuning vs true detuning
- 4 mechanical modes and 4% added noise
- Test error of about 4%. The accuracy of the training depends only on noise, regardless of the number of mechanical modes used

$$\varepsilon = \frac{\|(X' - WK)_n\|_F}{\|X'_n\|_F}$$

Model Predictive Control

Define Objectives

$$
\begin{aligned}
Y_{\text{target}} &= [V_r \; V_i \; \Delta\omega] \\
V_{cav} &= [V_r \; V_i \,] \\
\Delta\omega &= 0
\end{aligned}
$$

Model Predictive Control

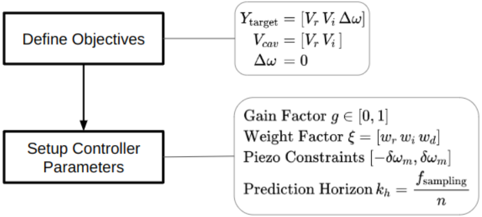

- A weight factor vector ξ is included to weight each objective of Y_{target}
- Piezo constraints are set to bound the maximum frequency shift per step, to account for the limited bandwidth of a real piezo actuator

Model Predictive Control

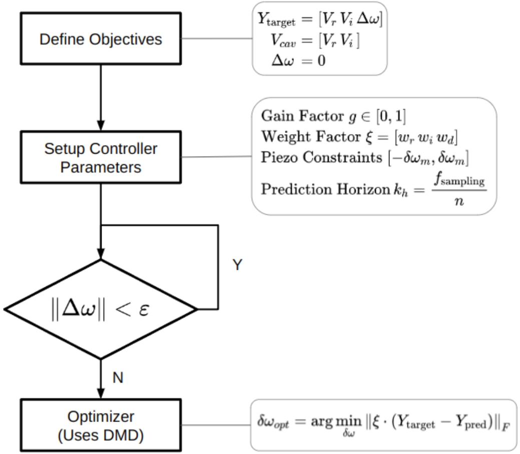

- A weight factor vector ξ is included to weight each objective of Y_{target}
- Piezo constraints are set to bound the maximum frequency shift per step, to account for the limited bandwidth of a real piezo actuator
- The optimizer performs a basic grid search over the possible values of the piezo. The value that minimizes the cost function is selected as the optimal.

$$\delta\omega \in [-\delta\omega_{\text{max}}, \delta\omega_{max}]$$

Model Predictive Control

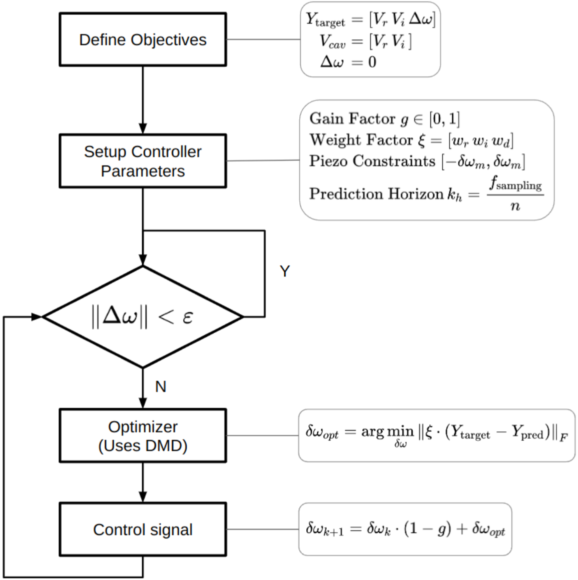

- A weight factor vector ξ is included to weight each objective of Y_{target}
- Piezo constraints are set to bound the maximum frequency shift per step, to account for the limited bandwidth of a real piezo actuator
- The optimizer performs a basic grid search over the possible values of the piezo. The value that minimizes the cost function is selected as the optimal.

$$\delta\omega \in [-\delta\omega_{\text{max}}, \delta\omega_{max}]$$

- Gain factor g included to generate a smooth control signal

Model Predictive Control

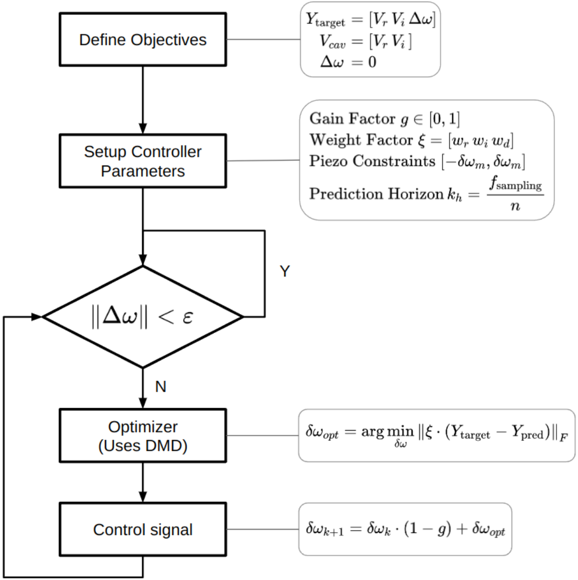

- A weight factor vector ξ is included to weight each objective of Y_{target}
- Piezo constraints are set to bound the maximum frequency shift per step, to account for the limited bandwidth of a real piezo actuator
- The optimizer performs a basic grid search over the possible values of the piezo. The value that minimizes the cost function is selected as the optimal.

$$\delta\omega \in [-\delta\omega_{\text{max}}, \delta\omega_{max}]$$

- Gain factor g included to generate a smooth control signal
- MPC requires extensive computation. Thus, the controller's complexity needs to be reduced. We use a lightweight model based on dynamic mode decomposition.

MPC performance

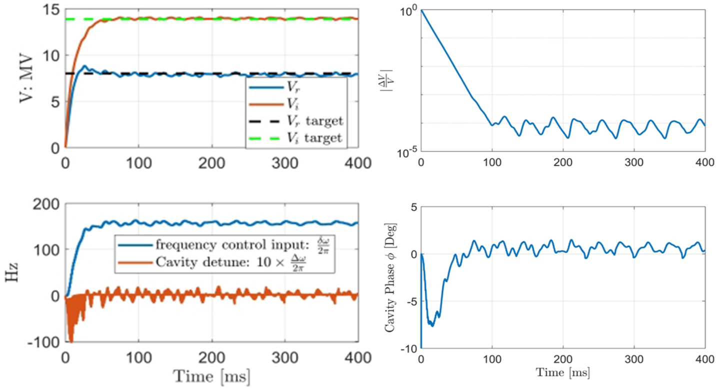

- Amplitude stability to 10^{-4}
- Phase stability to less than 1 degree
- Cavity detune less than 10 Hz
- 8 mechanical modes with 1% added noise.

Data Acquisition

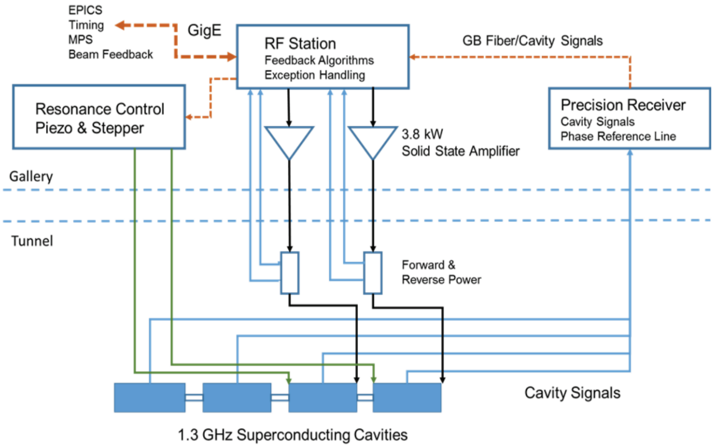

- Synchronized RF and piezo waveforms are needed to train the DMD model
- For the LCLS-II system, RF and piezo waveforms are digitized in separate chassis
- There is a communication protocol, over fiber links, between RFS and RES
- We included a global timing ID in the message to time-align RF and piezo signals
- For more information about the implementation check the poster ”FW/SW framework for SRF cavity active resonance control” by M. Donna

Data Acquisition

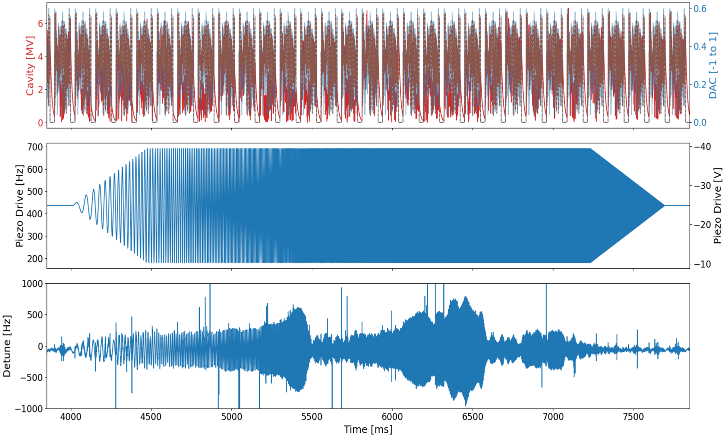

To maximize the hidden features extracted by the DMDc model, it is essential to diversify the data as much as possible. This is achieved by randomizing the driving RF and using a chirp for the piezo drive.

- RF drive should cover the operational range
- Piezo drive frequency should cover the range of microphonics, up to 200*Hz*
- Piezo drive amplitude greater than cavity bandwidth, 300*Hz*
- Sampling rate much higher than possible disturbance frequency. $f_s = 16kHz$
- RF and piezo control loops disabled

Data Acquisition

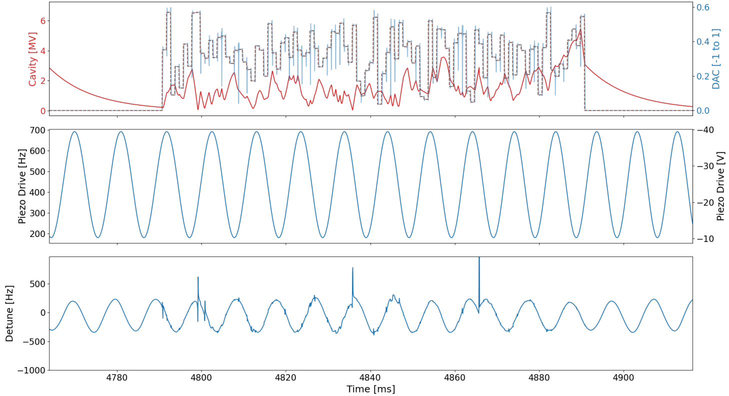

- To overcome computational burden, we use the ”almost linearly dependent” test
- The training dataset becomes a sparse subset of samples that spans the largest subspace in the data
- From the total dataset only 2% of samples are used for training
- We have collected data for CM20 cavities 8 and 7, and CM19 cavities 1 and 2

DMD predictions using cavity data

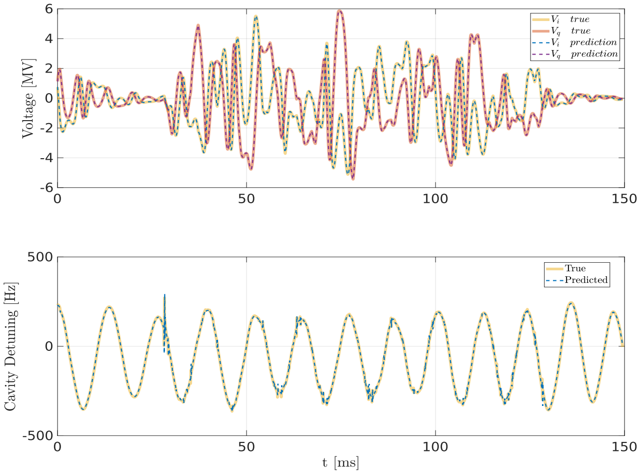

- Predicted cavity voltage vs true voltage. Real and imaginary components
- Predicted cavity detuning vs true detuning
- Test error less than 3%
- Data from each cavity is needed to train individual models for each cavity

Summary, Conclusions and Future Work

- Data-driven DMD model represents SRF cavity nonlinear dynamics and predicts the future state of the cavity. This has been demonstrated with LCLS-II cold cavities
- MPC simulations show promising results toward the development of a data-driven SRF resonance controller
- We are working on the implementation of the controller on an LCLS-II LLRF resonance control system
- The work presented here is not limited to resonance control, it can be adapted to the stabilization of quadrupole magnets, beamlines, and other systems that have coupling between external vibrational sources and the accelerator

Acknowledgements

Thanks to the LCLS-II LLRF team and the SRF team at SLAC, and thanks to the LLRF team at LBNL.

References

[1] PETER J. SCHMID. "Dynamic mode decomposition of numerical and experimental data". In: *Journal of Fluid Mechanics* 656 (2010), pp. 5–28. DOI: 10.1017/S0022112010001217.

[2] Peter J. Baddoo et al. "Kernel learning for robust dynamic mode decomposition: linear and nonlinear disambiguation optimization". In: *Proceedings of the Royal Society A: Mathematical, Physical and Engineering Sciences* 478.2260 (2022), p. 20210830. DOI: 10.1098/rspa.2021.0830.

[3] Faya Wang. "Enhancing SRF cavity stability and minimizing detuning with data-driven resonance control based on dynamic mode decomposition". In: *AIP Advances* 13.7 (July 2023), p. 075104. DOI: 10.1063/5.0154213.

THANK YOU

감사합니다

LCLS-II Microphonics

CM19 cavities 1 and 2 are gradient-limited (12 MV/cavity) due to microphonics. The main sources of microphonics are liquid helium valve regulation, vacuum pumps, and cool-down valve leaks.

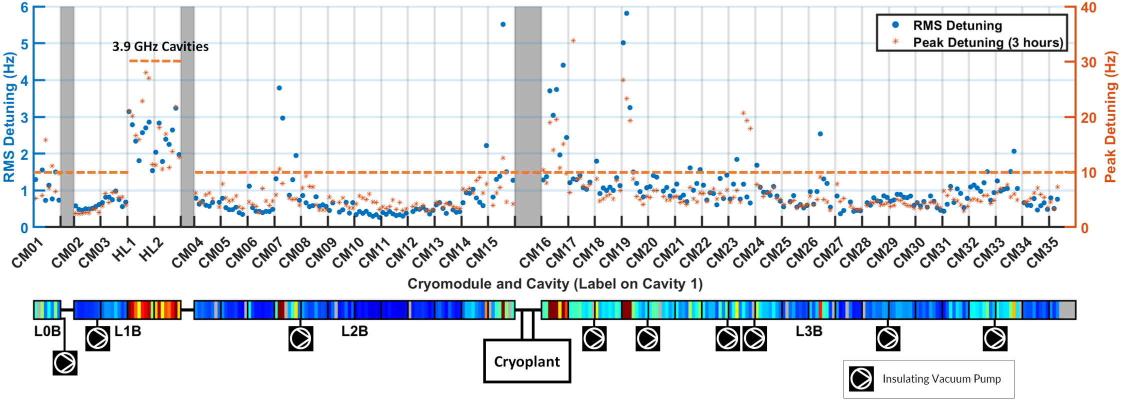

Courtesy of Ryan Porter

LCLS-II Resonance Control Firmware